RADIAITON AND CHEMICAL REACTION EFFECT ON MHD ACCELERATED INCLINED PLATE WITH VARIABLE TEMPERATURE

[1]D Chenna Kesavaiah, [2]D Chandraprakash

[1]Department of Humanities & Science, K G Reddy College of Engineering & Technology, Chilkur (V), Moinabad (M), R R Dist, Pin: 501504, TS, India
Email: chennakesavaiah@gmail.com

[2]Department of Electronics and Communication Engineering, K G Reddy College of Engineering & Technology, Chilkur (V), Moinabad (M), R R Dist, Pin: 501504, TS, India

Abstract **- An unsteady MHD free convection flow, heat and mass transfer past an exponentially accelerated inclined plate embedded in a saturated porous medium with uniform permeability, variable temperature and concentration has been carried out. An inexpensive of the present study was to analyze the effect of angle of inclination on the flow phenomena in the presence of heat source and destructive reaction. The perturbation method has been used to solve the governing equations. The effects of various parameters on velocity profiles, temperature profiles, concentration profiles, skin friction, Nusselt number and Sherwood number are shown graphically by using MATLAB. The present study has an immediate application in understanding the drag experienced at the heated/cooled and inclined surfaces in a seepage flow.**

Keywords*: Radiation, Magnetic field, Chemical reaction, Heat Source, Variable temperature*

I. INTRODUCTION

The application of electromagnetic fields in controlling the heat transfer as in aerodynamic heating lead to the study of magnetohydrodynamic heat transfer. This MHD heat transfer has gained significance owning to recent advancement of space technology. The MHD heat transfer can be divided into two sections. One contains problems in which heating is an incidental bi-product of the electromagnetic fields as in MHD generators, pumps etc. The second consists of problems in which the primary use of electromagnetic fields is to control heat transfer. Liquid in the geothermal region is an electrically conducting liquid because of high temperature. Hence the study of the interaction of the geomagnetic field with the fluid in the geothermal region is of great interest, thus leading to the study of MHD convection flow through a porous medium. Srinathuni Lavanya and Chenna Kesavaiah [1] Heat transfer to MHD free convection flow of a viscoelastic dusty gas through a porous medium with chemical reaction, Srinathuni Lavanya and Chenna Kesavaiah [2] Radiation effects on MHD natural convection heat transfer flow from spirally enhanced wavy channel through a porous medium, Chenna Kesavaiah and Sudhakaraiah [4] Effects of Heat and Mass Flux to MHD Flow in Vertical Surface with Radiation Absorption, Ch Kesavaiah et.al. [5] Effects of the chemical reaction and radiation

absorption on an unsteady MHD convective heat and mass transfer flow past a semi-infinite vertical permeable moving plate embedded in a porous medium with heat source and suction,

The influence of magnetic field on viscous incompressible flow of electrically conducting, radiative reactive fluid through porous medium associated with heat and mass transfer playing a key role in different areas of science and technology. The convective hence at and mass transfer flow in porous medium find several applications in many branches of science and technology like chemical industry, cooling of nuclear reactions, MHD power generators, geothermal energy extractions processes, petroleum engineering ect. in view these some of the authors studies Chenna Kesavaiah and Jahagirdar [3] observed MHD Free Convective Flow through Porous Medium under the Effects of Radiation and Chemical reaction, Hari Krishna et.al. [6] Effect of radiation and chemical reaction on MHD flow past an oscillating inclined porous plate with variable temperature and mass diffusion, Noor et.al. [7] Analyzed heat and mass transfer of thermophoretic MHD flow over an inclined radiative isothermal permeable surface in the presence of heat source/sink. Rajput and Gaurav Kumar [8] Chemical reaction effect on unsteady MHD flow past an impulsively started oscillating inclined plate with variable temperature and mass diffusion in the presence of hall current, Devika et.al. [9] Studied MHD oscillatory flow of a viscoelastic fluid in a porous channel with chemical reaction, Muthuraj et.al. [10] Influences of chemical reaction and wall properties on MHD peristaltic transport of dusty fluid with heat and mass transfer.

Chemical reactions are of importance in many practical processes such as hydrometallurgical industries and chemical technology such as polymer production and food processing distribution of temperature and moisture over agricultural field, energy transfer in a wet cooling tower, in method of generating and extracting power from a moving fluid, fluids undergoing exothermic or endothermic chemical reaction. These processes are observed in nuclear reactor safety and combustion systems, solar collectors, as well as metallurgical and chemical engineering. Due to the fast growth of electronic technology, effective cooling of electronic equipment has become warranted and cooling of electronic equipment ranges from individual transistors to main frame computers and from energy suppliers to telephone switch boards and thermal diffusion effect has been utilized for isotopes separation in the mixture between gases with very light molecular weight and medium molecular weight. Their other applications include solidification of binary alloys and crystal growth dispersion of dissolved materials or particulate water in flows, drying and dehydration operations in chemical and food processing plants, and combustion of atomized liquid fuels. Many transport processes that are governed by the combined action of buoyancy forces due to both thermal and mass diffusion in the presence of the chemical reaction effect. Some of the authors studied regarding this Chenna Kesavaiah and Venkateswarlu [11] studied chemical reaction and radiation absorption effects on convective flows past a porous vertical wavy channel with travelling thermal waves, Chenna Kesavaiah et.al. [12] Considered forced convective heat flow of a liquid

for different depths of the channel with a constant heat source, Chenna Kesavaiah et.al. [13] Examined MHD rotating fluid past a moving vertical plate in the presence of chemical reaction, Chenna Kesavaiah et.al. [14] Discussed radiation effect on slip flow regime with heat generation, Makinde and Ogulu [15] studied the effect of thermal radiation on the heat and mass transfer flow of a variable viscosity fluid past a vertical porous plate permeated by a transverse magnetic field, Mehari Fentahun Endalew and Anita Nayak [16] considered thermal radiation and inclined magnetic field effects on MHD flow past a linearly accelerated inclined plate in a porous medium with variable temperature, Ismail et.al. [17] The effects of magnetohydrodynamic and radiation on flow of second grade fluid past an infinite inclined plate in porous medium, England and Emery [18] Thermal radiation effects on the laminar free convection boundary layer of an absorbing gas, Pattnaik et.al. [19] Radiation and mass transfer effects on MHD flow through porous medium past an exponentially accelerated inclined plate with variable temperature, Rajput and Kumar [20] Radiation effects on MHD flow past an impulsively started vertical plate with variable heat and mass transfer.

The objective of the present paper is an unsteady MHD free convection flow, heat and mass transfer past an exponentially accelerated inclined plate embedded in a saturated porous medium with uniform permeability, variable temperature and concentration has been carried out. An inexpensive of the present study was to analyze the effect of angle of inclination on the flow phenomena in the presence of heat source/sink and destructive reaction. The velocity, temperature and concentration are shown graphically for various premasters involving in governing differential equations.

II. FORMULATION OF THE PROBLEM

We consider an unsteady uniform MHD free convective flow of a viscous, incompressible and radiating fluid past an exponentially accelerated inclined plate with variable temperature embedded in a saturated porous medium. The x – axis is taken along the plate and y –axis is normal to the plate. Magnetic field intensity B_0 is applied in the direction perpendicular to the plate. The plate is inclined to vertical direction by an angle c. the induced magnetic field is neglected as the magnetic Reynolds number of the flow is very small. Initially, it is assumed that the plate and the surrounding fluid are at the same temperature T_∞ and the concentration C_∞ and the physical model of the problem shown in figure (1).

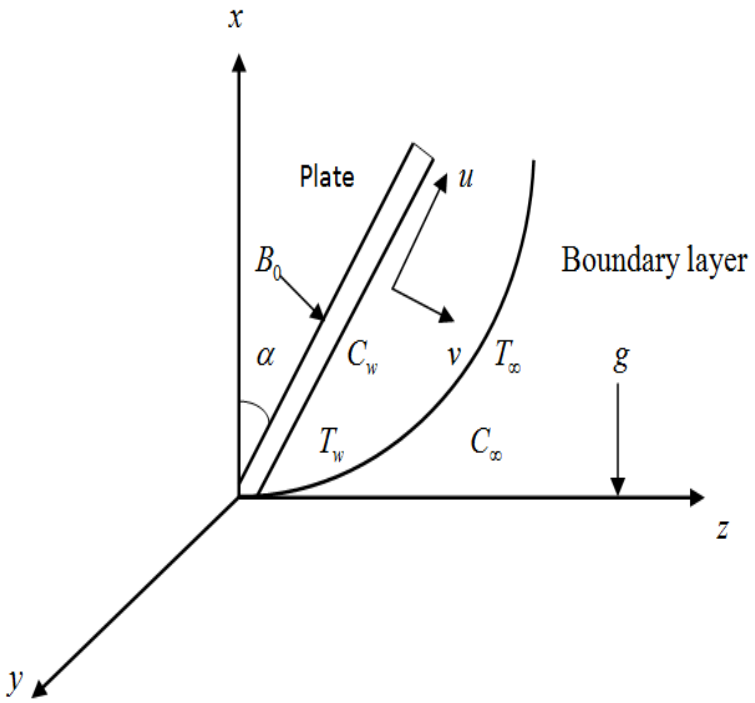

Figure (1): Physical mode of the problem

In view of the above the boundary layer equations of flow, heat and mass transfer past an exponentially accelerated inclined plate are given by

$$\frac{\partial u}{\partial t}=\nu\frac{\partial^2 u}{\partial z^2}+g\,\beta\left(T-T_\infty\right)\cos\alpha+g\,\beta^*\left(C-C_\infty\right)\cos\alpha-\frac{\sigma B_0^2\left(u+mv\right)}{\rho\left(1+m^2\right)}-\frac{\nu}{K}u \tag{1}$$

$$\frac{\partial v}{\partial t}=\nu\frac{\partial^2 v}{\partial z^2}+\frac{\sigma B_0^2\left(mu-v\right)}{\rho\left(1+m^2\right)}-\frac{\nu}{K}v \tag{2}$$

$$\frac{\partial T}{\partial t}=\frac{\kappa}{\rho C_p}\frac{\partial^2 T}{\partial z^2}-\frac{1}{\rho C_p}\frac{\partial q_r}{\partial z}-\frac{Q_0}{\rho C_p}\left(T-T_\infty\right) \tag{3}$$

$$\frac{\partial C}{\partial t}=\kappa\frac{\partial^2 C}{\partial z^2}-K_r\left(C-C_\infty\right) \tag{4}$$

The initial and boundary conditions are:

$$u=0,v=0,T=T_\infty,C=C_\infty\quad,t\le 0$$

$$\left.\begin{array}{ll} u=u_0\cos\omega t,v=0,T=T_\infty+\dfrac{\left(T_\omega-T_\infty\right)u_0^2 t}{\nu},C=C_\infty+\dfrac{\left(C_w-C_\infty\right)u_0^2 t}{\nu}\,at & z=0\\ u\to 0,v\to 0,T\to T_\infty,C\to C_\infty & as\ z\to\infty \end{array}\right\},t>0 \tag{5}$$

Here $u-$ is the primary velocity, $v-$ the secondary velocity, $g-$the acceleration due to gravity, $\beta-$volumetric coefficient of thermal expansion, $t-$time, $m\left(=\omega_e\tau_e\right)$ the hall current parameter with ω_e cyclotron frequency of electrons and electron collision of time, $T-$temperature of the fluid, β^*-volumetric coefficient, $C-$spices concentration, $\nu-$kinematic viscosity, $\rho-$the density, $C_p-$the

specific heat, $\kappa-$thermal conductivity of the fluid, $D-$the mass diffusion coefficient, $K-$the permeability parameter, T_w-temperature of the plate at $z=0$, C_w species concentration at $z=0$, B_0 the plate the uniform magnetic field, $\sigma-$electrical conductivity.

The boundary conditions for the temperature at the plate impose a linearity relation between temperature and time with a residual temperature T_∞ and having a constant slope $\frac{u_0^2}{\nu}$ which depends upon square of the characteristic velocity and material property. Similar explanation holds for concentration at the plate. The fluid considered here is a gray, absorbing/emitting radiation but a non-scattering medium. The local gradient for the case of an optically thin gray gas is expressed by

$$\frac{\partial q_r}{\partial z}=-4a^*\sigma\left(T_\infty{}^4-T^4\right) \tag{6}$$

We assumed that the temperature differences within the flow are sufficiently small such that T^4 may be expressed as a linear function of the temperature. This is accomplished by expanding T^4 in a Taylor series about T_∞ and neglecting the higher order terms, we get

$$T^4\cong 4T_\infty{}^4T-3T_\infty{}^4 \tag{7}$$

Using equation (6) and (7) we have

$$\rho C_p\frac{\partial T}{\partial z}=\kappa\frac{\partial^2T}{\partial z^2}-16a^*T_\infty{}^3\sigma\left(T-T_\infty\right)-Q_0\left(T-T_\infty\right) \tag{8}$$

On introducing the following non – dimensional quantities

$$z^*=\frac{zu_0}{\nu},u^*=\frac{u}{u_0},v^*=\frac{v}{v_0},t^*=\frac{tu_0{}^2}{\nu},\omega^*=\frac{\omega\nu}{u_0^2},T=\frac{T-T_\infty}{T_w-T_\infty},\ C=\frac{C-C_\infty}{C_w-C_\infty}$$
$$Gr=\frac{\nu\beta g\left(T_w-T_\infty\right)}{u_0{}^3},\quad \Pr=\frac{\mu C_p}{\kappa},\quad Gc=\frac{\nu\beta^*g\left(C_w-C_\infty\right)}{u_0{}^3},\quad M=\frac{\sigma B_0{}^2\nu}{\rho u_0{}^2} \tag{9}$$
$$K^*=\frac{Ku_0{}^2}{\nu^2},\quad Kr^*=\frac{Kr\,\nu}{u_0{}^2},\quad R=\frac{16a^*\nu^2\sigma T_\infty}{\kappa u_0{}^2},\quad Q=\frac{Q_0\nu}{\rho C_p u_0{}^2},\quad Sc=\frac{\nu}{D}$$

where $Gr-$thermal Grashof number, $Gc-$mass Grashof number, $K-$the dimensionless permeability parameter, $\Pr-$the Prandtl number, $Sc-$the Schmidt number, $R-$radiation parameter, $M-$the magnetic parameter and $Q-$ is heat source/sink parameter

The basic field equations (1) – (4) can be expressed in the non – dimensional from and dropping the starts $(*)$ as

$$\frac{\partial u}{\partial t}=\frac{\partial^2u}{\partial z^2}+Gr\cos\alpha\ \theta+Gc\ \cos\alpha\ \theta-\frac{M\left(u+mv\right)}{1+m^2}-\frac{1}{K}u \tag{10}$$

$$\frac{\partial v}{\partial t}=\frac{\partial^2v}{\partial z^2}+\frac{M\left(mu-v\right)}{1+m^2}-\frac{1}{K}v \tag{11}$$

$$\frac{\partial \theta}{\partial t} = \frac{1}{\Pr}\frac{\partial^2 \theta}{\partial y^2} - \left(\frac{R}{\Pr} + Q\right)\theta \tag{12}$$

$$\frac{\partial C}{\partial t} = \frac{1}{Sc}\frac{\partial^2 C}{\partial z^2} - Kr\ C \tag{13}$$

The initial and boundary conditions in dimensionless form are

$$\left.\begin{array}{ll} u = 0, v = 0, \theta = 0, C = 0 & t \le 0 \quad for\ all\ \ z \\ u = \cos \omega t, v = 0, \theta = t, C = t, & at\ \ z = 0 \\ u = 0, v \to 0, \theta \to 0, C \to 0 & as\ \ z \to \infty \end{array}\right\} \quad t > 0 \tag{14}$$

Combining the equations (10) and (11), the model becomes

$$\frac{\partial q}{\partial t} = \frac{\partial^2 q}{\partial z^2} + Gr \cos\alpha\ \theta + Gc\ \cos\alpha\ \theta - \left(\frac{M(1-im)}{1+m^2} + \frac{1}{K}\right)q \tag{15}$$

Finally the boundary becomes

$$\left.\begin{array}{ll} q = 0, , \theta = 0, C = 0 & t \le 0 \quad for\ all\ \ z \\ q = \cos \omega t, \theta = t, C = t, & at\ \ z = 0 \\ q \to 0, \theta \to 0, C \to 0 & as\ \ z \to \infty \end{array}\right\} \quad t > 0 \tag{16}$$

wehre $q = u + iv$

III. SOLUTION OF THE PROBLEM

Equation (12), (13) and (15) are coupled, non – linear partial differential equations and these cannot be solved in closed – form using the initial and boundary conditions (16). However, these equations can be reduced to a set of ordinary differential equations, which can be solved analytically. This can be done by representing the velocity, temperature and concentration of the fluid in the neighbourhood of the fluid in the neighbourhood of the plate as

$$\begin{aligned} q(z,t) &= q_0(z)\ e^{i\omega t} \\ \theta(z,t) &= \theta_0(z) e^{i\omega t} \\ C(z,t) &= C_0(z) e^{i\omega t} \end{aligned} \tag{17}$$

Substituting (17) in Equation (15), (12), (13) and equating the harmonic and non – harmonic terms, we obtain

$$q_0'' - \beta_3^2 q_0 = -Gr \cos\alpha\ \theta_0 - Gc \cos\alpha\ C_0 \tag{18}$$

$$\theta_0'' - \beta_2^2\ \theta_0 = 0 \tag{19}$$

$$C_0'' - \beta_1^2 C_0 = 0 \tag{20}$$

here the summits denote the differentiation w. r. t. y

where $\beta_1^2 = (Kr + i\omega)Sc, \beta_2^2 = (R - Q\Pr + i\omega \Pr), \beta_3^2 = \left[\frac{M(1-im)}{1+m^2} + \frac{1}{K}\right]$

The corresponding boundary conditions can be written as

$$q_0 = e^{-i\omega t}\cos\omega t, \quad \theta_0 = t\,e^{-i\omega t}, C_0 = t\,e^{-i\omega t} \qquad at\ z = 0$$
$$q_0 \to 0, \qquad \theta_0 \to 0, \quad C_0 \to 0 \qquad as\ z \to \infty \qquad (21)$$

Solving Equations (18) - (20) under the boundary conditions (21) and we obtain the velocity, temperature and concentration distributions in the boundary layer as

$$q_0 = Y_1 e^{-\beta_2 z} + Y_2 e^{-\beta_1 z} + Y_3 e^{-\beta_3 z}$$

$$\theta_0 = t\ e^{-i\omega t - \beta_2 z}$$

$$C_0 = t\ e^{-i\omega t - \beta_1 z}$$

In view of the equation (17) becomes

$$q = e^{i\omega t}\left\{Y_1 e^{-\beta_2 z} + Y_2 e^{-\beta_1 z} + Y_3 e^{-\beta_3 z}\right\}$$

$$\theta = e^{i\omega t}\left\{t\ e^{-i\omega t - \beta_2 z}\right\}$$

$$C = e^{i\omega t}\left\{t\ e^{-i\omega t - \beta_1 z}\right\}$$

Coefficient of Skin-Friction

The coefficient of skin-friction at the vertical porous surface is given by

$$C_f = \left(\frac{\partial q}{\partial z}\right)_{z=0} = e^{i\omega t}\left\{Y_1\beta_2 + Y_2\beta_1 + Y_3\beta_3\right\}$$

Coefficient of Heat Transfer

The rate of heat transfer in terms of Nusselt number at the vertical porous surface is given by

$$N_u = \left(\frac{\partial \theta}{\partial z}\right)_{z=0} = e^{i\omega t}\left\{t\ \beta_2 e^{-i\omega t}\right\}$$

Sherwood number

$$Sh = \left(\frac{\partial C}{\partial z}\right)_{z=0} = e^{i\omega t}\left\{t\ \beta_1 e^{-i\omega t}\right\}$$

IV. RESULTS AND DISCUSSIONS

The effect of thermal Grashof number (Gr) on the velocity is exposed in Fig. 2 the thermal Grashof number shows the qualified result of the thermal buoyancy force to the viscous hydraulics force. The flow is quicker as a result of the event in buoyancy force matching to a growth within the thermal Grashof number. Heat is so conducted aloof from the vertical plate into the fluid will increase the temperature and thereby enhance the buoyancy force. Additionally, it is seen that the values of the velocity improve quickly close to the plate as thermal Grashof number will increase so disintegrates swimmingly to stream velocity. Fig. 3 shows velocity profiles within the physical phenomenon for different solutal Grashof number (Gc), we observe that the velocity will increase with increasing values of the solutal Grashof number. Fig. 4 displays the consequences of angle of disposition (α) on the velocity profiles. It is pragmatic that the

velocity reduces for positive change in the angle of inclination α. Fig. 5 shows the results of the permeability on the velocity profiles and the velocity increases with the increasing dimensionless porous parameter. Fig. 6, plotted the behaviour velocity profiles for various values of chemical reaction parameter, it is ascertained that a rise in results in a decrease in each the values of velocity. A definite velocity increase happens close to the wall when that profiles decay swimmingly to the stationary price in free stream. Hence the chemical action accelerates the flow. Fig. 7 depicts the results of the Hall current parameter (m) on the velocity profiles, it is ascertained that for lower values of Hall current parameter, the velocity will increase for increasing Hall current parameter**.** Fig. 8 signifies the velocity outlines for various principles of magnetic parameter (M) in the figure; it ascertained that the velocity decrease with improvement of the magnetic parameter. Fig. 9, illustrates the characteristic of velocity profiles for various values of Prandtl number (Pr). It is noticed that a rise within the Prandtl number results in reduction of the thermal thickness. This is due to the fact that fluid with large Prandtl number has high viscosity and small thermal conductivity, which make the fluid thick and causes a decrease in fluid velocity. The influence of presence of the heat source parameter (Q) on the velocity distribution in the boundary layer is presented in Fig. 10. It is obvious that increasing the values of heat source parameter produces a decrease in the velocity distribution of the fluid. This is expected since the presence of a heat sink in the boundary layer absorbs energy. Which in turn cause the temperature of the fluid to decreases. This decrease in temperature produces a decrease in the flow field due to the buoyancy effect which couples the flow and thermal field. The consequences of radiation parameter (R) on velocity are unit shown in Fig. 11 respectively. It is seem that the velocity declines with a growing the radiation parameter. Fig. 12 shows the effect of Schmidt number on the velocity profiles for $Sc = 0.16$ (hydrogen), $Sc = 0.3$ (helium), $Sc = 0.6$ (water vapour), $Sc = 2.01$ (ethyl Benzene). It is observed that the velocity decreases with increasing Schmidt number values due to the decrease in the molecular diffusivity, which results in a decrease in the concentration and velocity boundary layer thickness. Variation of velocity profiles for different values of dimensionless time parameter (t) is shown in Fig. 13. It is noticed that the velocity decreases with the progression of time. The velocity profiles for different values angle of inclination (ω) is shown in Fig. 14. It is noticed that the velocity decreases with the progression of ω. Fig. 15 illustrate the characteristic of temperature profiles for various values of Prandtl number (Pr). It is noticed that a rise within the Prandtl number results in reduction of the thermal thickness and generally lower average temperature among the physical phenomenon, the reason for that smaller values of area unit admire increase within the thermal conduction of the fluid and thus, heat will diffuse aloof from the heated surface earlier for higher values of Prandtl number. Fig. 16 has been plotted to depict the variation of temperature

profiles against y for different values of heat source parameter (Q) by fixing other parameter. It is observed from this graph that temperature increase with increasing heat source parameter. It is observed in Fig. 17 that the temperature (θ) increases as the radiation parameter (R) decreases in the temperature. The effects of time parameter (t) and angle of inclination (ω) shown in Fig. 18 and Fig. 19, it is observed that the increases in time parameter the temperature increases, but increase in angle of inclination resulted in the decrease of the temperature. The effect of chemical reaction parameter (Kr) on the concentration (ϕ) is shown in Fig. 20. It is noticed from this figure that there is a marked effect of increasing values of on concentration distribution in the boundary layer. It is clearly observed from this figure that increasing values of decrease the concentration of species in the boundary layer. This happens because large values of chemical reaction parameter reduce the solutal boundary layer thickness and increase the mass transfer. The concentration profiles is shown in Fig. 21, increase in Schmidt number (Sc) shows that the concentration profiles reduce. This cause the concentration buoyancy effects to reduce yielding a reduction within the fluid velocity; reduction within the concentration distribution area unit in the simultaneous reduction within the concentration boundary layers. For different values of time parameter (t) are shown in Fig. 22, it is clear that the concentration increases with increases in time parameter, but the reverse effect observed for different values of angle of inclination parameter (ω), in Fig. 23. Skin friction is a measure of shearing stress experienced at the solid surface. Fig. 24 exhibit the effect of angle of disposition (α), it is observed that an increasing angle of dissipation the skin friction was decreased. From Fig. 25, it is observed that the absolute values of the rate of heat transfer decreases as the angle of inclination parameter (ω) increases versus different values with radiation parameter. From Fig. 26, it is observed that the absolute values of the rate of mass transfer decreases as the angle of inclination parameter (ω) increases versus different values with chemical reaction parameter.

Appendix

$$\beta_1 = \text{Real part of } \sqrt{(Kr + i\omega)Sc} = \sqrt{\frac{KrSc + Kr^2Sc^2 + \omega^2Sc^2}{2}}$$

$$\beta_2 = \text{Real part of } \left(R - Q\,\text{Pr} + i\omega\,\text{Pr}\right) = \sqrt{\frac{(R - Q\,\text{Pr}) + (R - Q\,\text{Pr})^2 + \omega^2\,\text{Pr}^2}{2}}$$

$$\beta_3 = \text{Real part of } \left[\frac{M(1 - im)}{1 + m^2} + \frac{1}{K}\right] = \sqrt{\frac{\frac{KM + 1 + m^2}{K(1 + m^2)} + \left(\frac{KM + 1 + m^2}{K(1 + m^2)}\right)^2 + \left(\frac{KMm}{K(1 + m^2)}\right)^2}{2}}$$

$$Y_1 = -\frac{Gr\ t\ \cos\omega t \cos\alpha}{\beta_2^{\,2} - \beta_3^{\,2}}, Y_2 = -\frac{Gc\ t\ \cos\omega t \cos\alpha}{\beta_1^{\,2} - \beta_3^{\,2}}, Y_3 = \left(\cos^2\omega t - Y_1 - Y_2\right)$$

REFERENCE

[1] Srinathuni Lavanya and D. Chenna Kesavaiah "Heat transfer to MHD free convection flow of a viscoelastic dusty gas through a porous medium with chemical reaction", *International Journal of Pure and Applied Researches*, vol. 3 (1), pp. 43 – 56, 2017.

[2] Srinathuni Lavanya and D. Chenna Kesavaiah "Radiation effects on MHD natural convection heat transfer flow from spirally enhanced wavy channel through a porous medium", *International Journal on Future Revolution in Computer Science & Communication Engineering*, vol. 3(10), pp. 130-140, 2017.

[3] D. Chenna Kesavaiah and R. S. Jahagirdar "MHD Free Convective Flow through Porous Medium under the Effects of Radiation and Chemical reaction", *Journal of Applied Science and Computations*, vol. 5 (10), pp. 1125-1140, 2018

[4] D. Chenna Kesavaiah and A. Sudhakaraiah "Effects of Heat and Mass Flux to MHD Flow in Vertical Surface with Radiation Absorption", *Scholars Journal of Engineering and Technology*, vol. 2 (2B): pp. 219-225, 2014

[5] D. Ch. Kesavaiah, P. V. Satyanarayana and S. Venkataramana "Effects of the chemical reaction and radiation absorption on an unsteady MHD convective heat and mass transfer flow past a semi-infinite vertical permeable moving plate embedded in a porous medium with heat source and suction", *Int. J. of Appl. Math and Mech.* vol. 7 (1), pp. 52-69, 2011

[6] Y. Hari Krishna, M. V. Ramana Murthy, N. L. Bhikshu and G. Venkataramana "Effect of radiation and chemical reaction on MHD flow past an oscillating inclined porous plate with variable temperature and mass diffusion", *International Journal of Chemical Sciences*, vol. 15 (3), pp. 1-12, 2017

[7] N. F. M. Noor, S. Abbas Bandy and I. Hashim "Heat and mass transfer of thermophoretic MHD flow over an inclined radiative isothermal permeable surface in the presence of heat source/sink", *Int. J. Heat Mass Transf.*, vol. 55 (2), pp. 22-28, 2012

[8] U. S. Rajput and Gaurav Kumar "Chemical reaction effect on unsteady MHD flow past an impulsively started oscillating inclined plate with variable temperature and mass diffusion in the presence of hall current", *Applied Research Journal*, vol. 2(5), pp. 244-253, 2016

[9] B. Devika et.al "MHD oscillatory flow of a viscoelastic fluid in a porous channel with chemical reaction", *International Journal of Engineering Science Invention*, vol. 2 (2), pp. 26-35, 2013

[10] R. Muthuraj, K. Nirmala and S. Srinivas "Influences of chemical reaction and wall properties on MHD peristaltic transport of \dusty fluid with heat and mass transfer, Alexandria Engineering Journal, vol. 55 (1), pp. 597-611, 2016

[11] D. Chenna Kesavaiah and B. Venkateswarlu "Chemical reaction and radiation absorption effects on convective flows past a porous vertical wavy channel with travelling thermal waves", *International Journal of Fluid Mechanics Research Accepted*, 2019

[12] D Chenna Kesavaiah, G Shanya Psalms and G Srujana "Forced convective heat flow of a liquid for different depths of the channel with a constant heat source", *Adalya Journal*, vol. 8 (7), pp. 15-22, 2019.

[13] D Chenna Kesavaiah, K Ramakrishna Reddy and G Priyanka Reddy "MHD rotating fluid past a moving vertical plate in the presence of chemical reaction", *International Journal of Information and Computing Science,* vol. 6 (2), pp. 142-154, 2019

[14] D Chenna Kesavaiah, Ikramuddin Sohail Md, R S Jahagirdar "Radiation effect on slip flow regime with heat generation", *Cikitusi Journal For Multidisciplinary Research*, vol. 6 (1), pp. 7-18, 2019

[15] O.D. Makinde and A. Ogulu " The effect of thermal radiation on the heat and mass transfer flow of a variable viscosity fluid past a vertical porous plate permeated by a transverse magnetic field", *Chemical Engineering Communications*, vol. 195 (12), pp. 1575-1584, 2008.

[16] Mehari Fentahun Endalew and Anita Nayak " Thermal radiation and inclined magnetic field effects on MHD flow past a linearly accelerated inclined plate in a porous medium with variable temperature", *Heat Transfer- Asian Res.*, vol. 8, pp. 42-61, 2019

[17] Z. Ismail, I. Khan N. M. Nasir, R.J. Wang, M. Z. Salleh, S. Shafie "The effects of magnetohydrodynamic and radiation on flow of second grade fluid past an infinite inclined plate in porous medium" *Proc AIP Conf*., VOL. 1643 (1), pp. 563-569, 2015.

[18] W. G. England and A. F. Emery "Thermal radiation effects on the laminar free convection boundary layer of an absorbing gas". *J Heat Trans*., vol. 91, pp. 37-44, 1969

[19] J. R. Pattnaik, G. C. Dash, S. Singh "Radiation and mass transfer effects on MHD flow through porous medium past an exponentially accelerated inclined plate with variable temperature". *Ain Shams Eng J.* Vol. 8, pp. 67-75, 2017

[20] U.S. Rajput, S. Kumar "Radiation effects on MHD flow past an impulsively started vertical plate with variable heat and mass transfer", *Int. J. Appl. Math. Mech*. Vol. 8 (1), pp. 66-85, 2012.

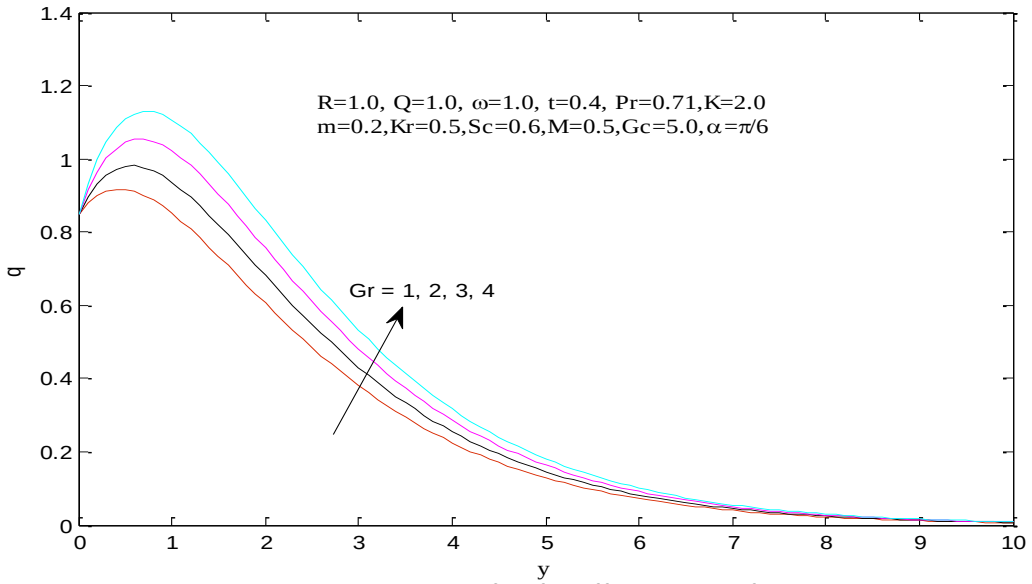

Fig. 2: Velocity profiles for different values of Gr

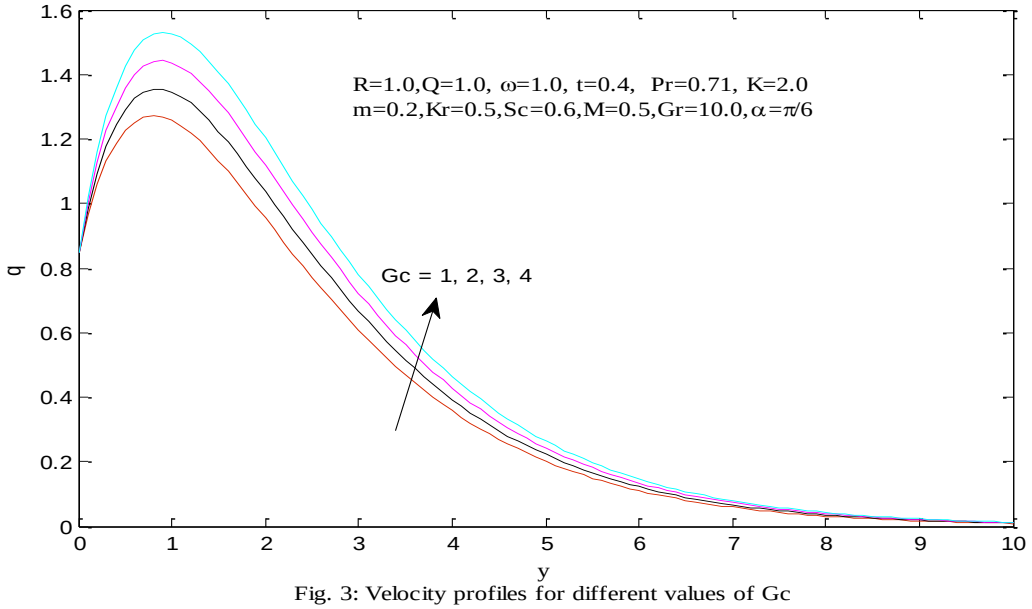

Fig. 3: Velocity profiles for different values of Gc

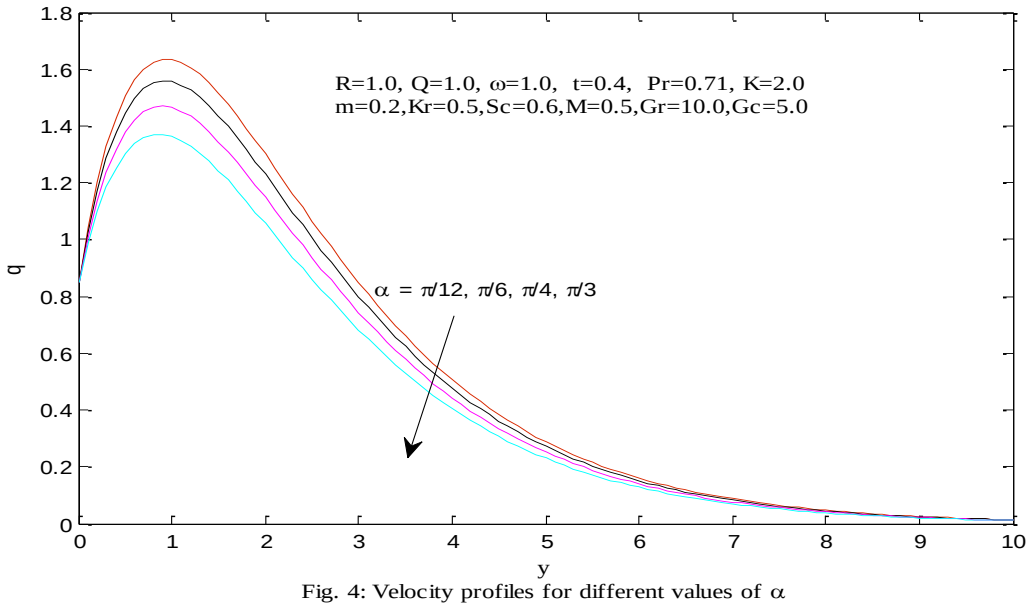

Fig. 4: Velocity profiles for different values of α

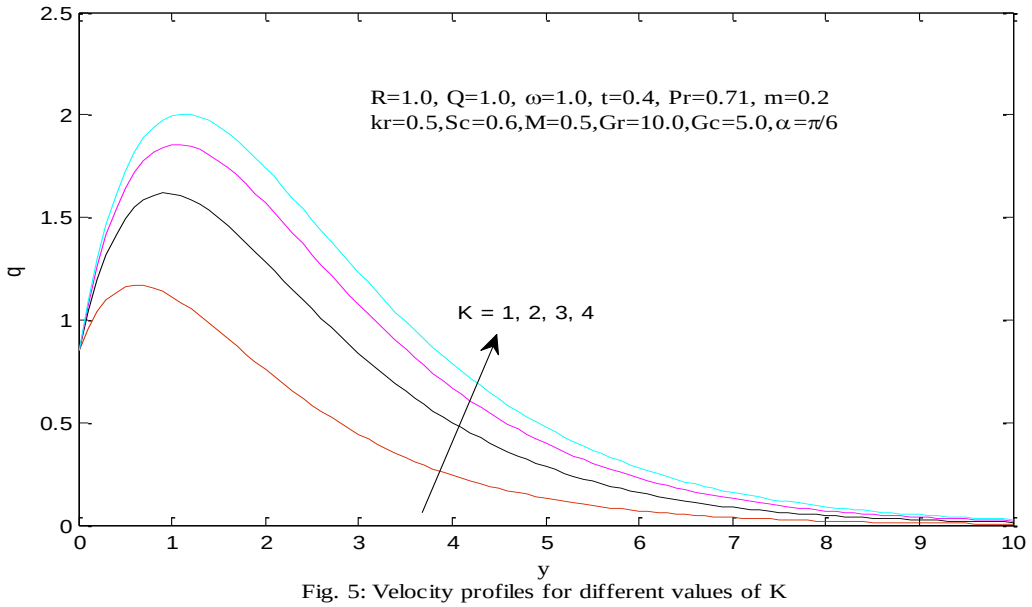

Fig. 5: Velocity profiles for different values of K

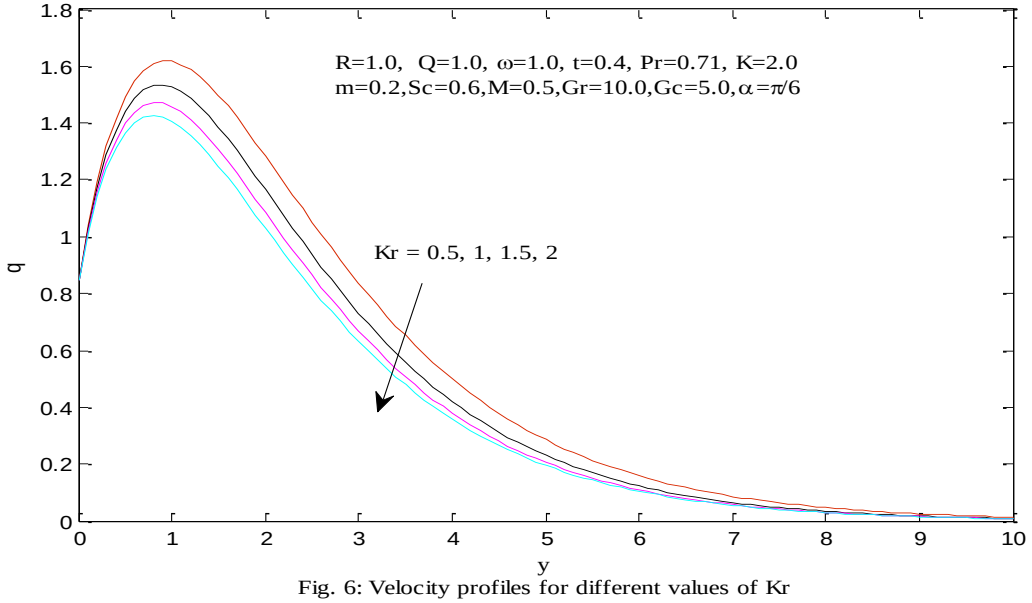

Fig. 6: Velocity profiles for different values of Kr

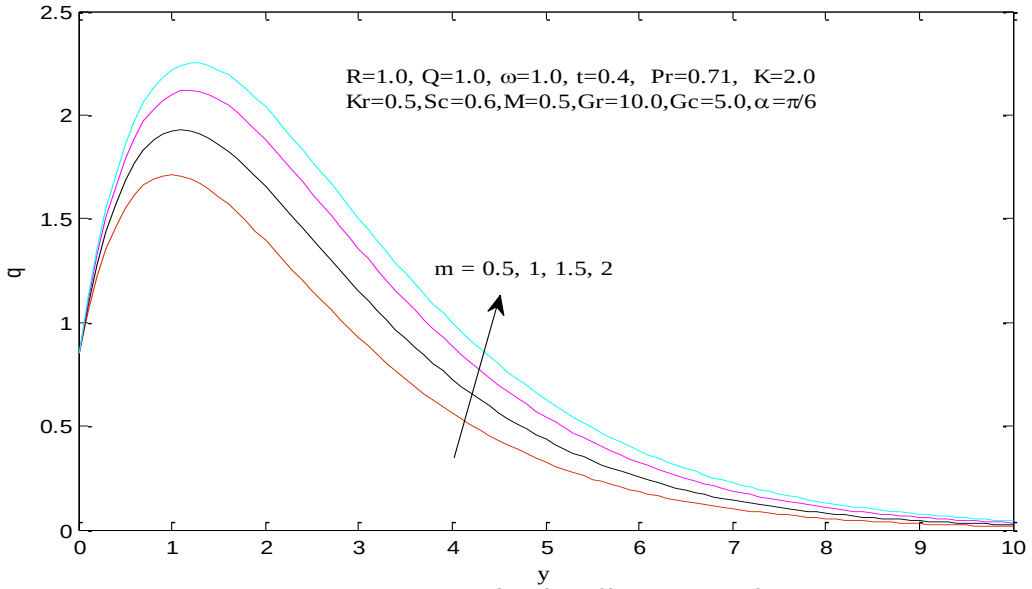

Fig. 7: Velocity profiles for different values of m

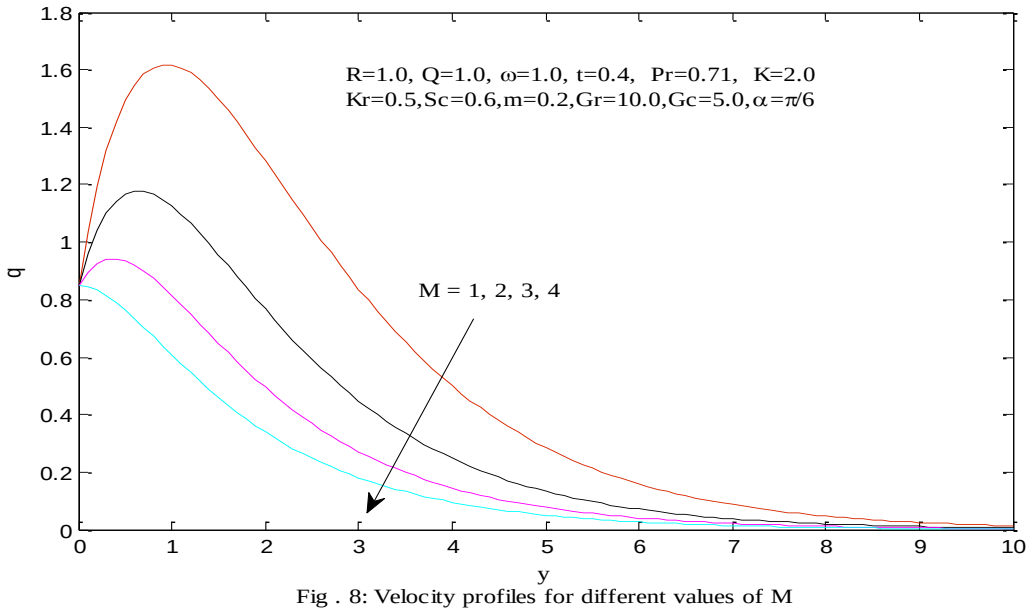

Fig . 8: Velocity profiles for different values of M

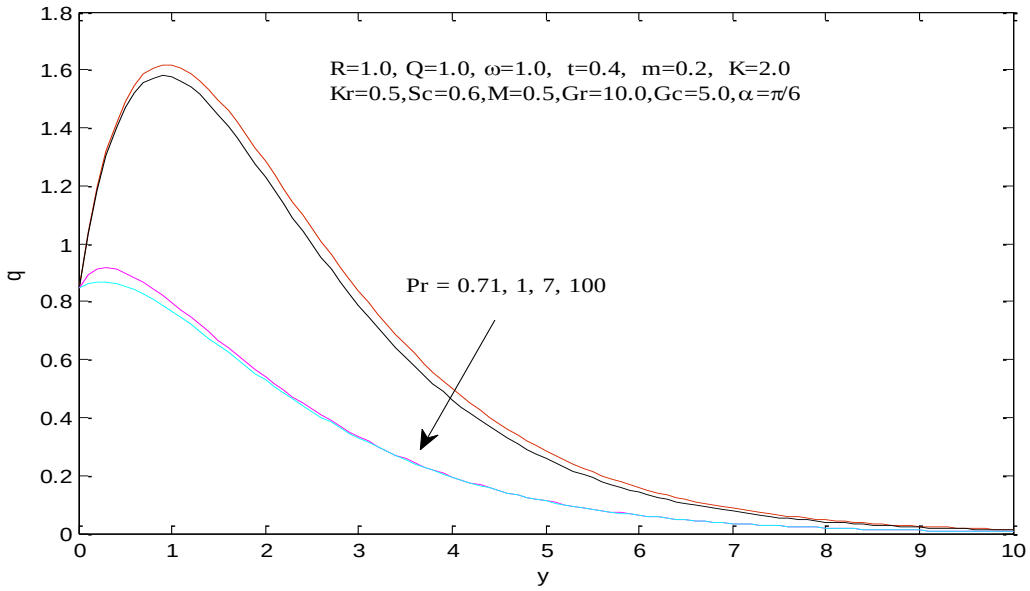

Fig. 9: Velocity profiles for different values of Pr

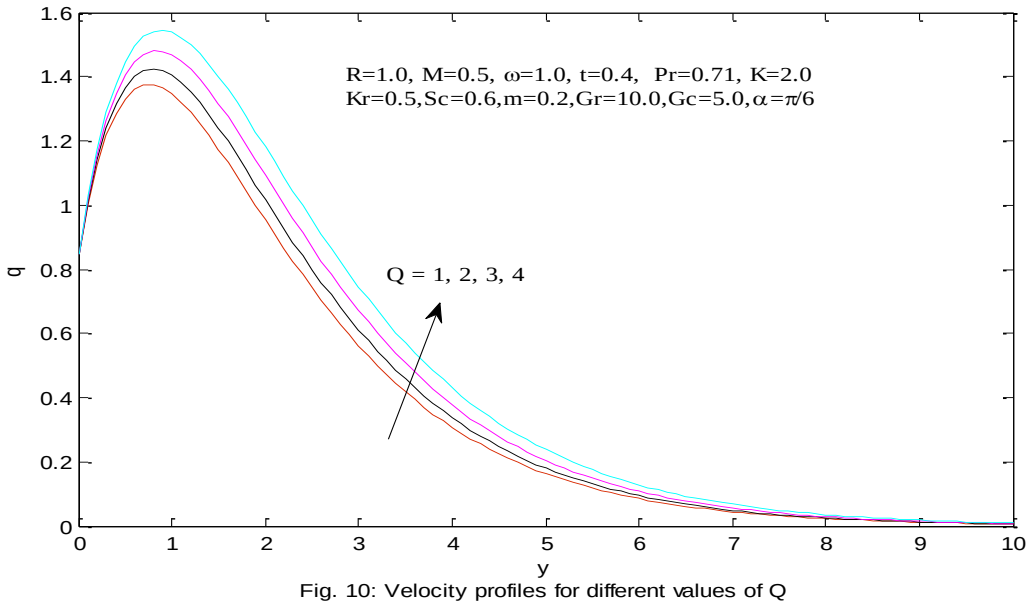

Fig. 10: Velocity profiles for different values of Q

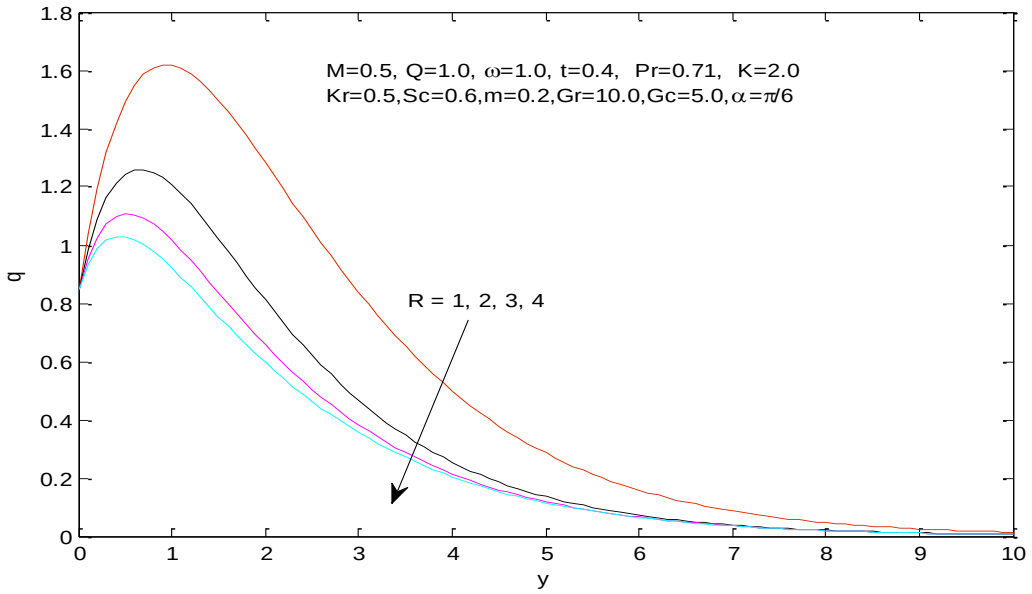

Fig. 11: Velocity profiles for different values of R

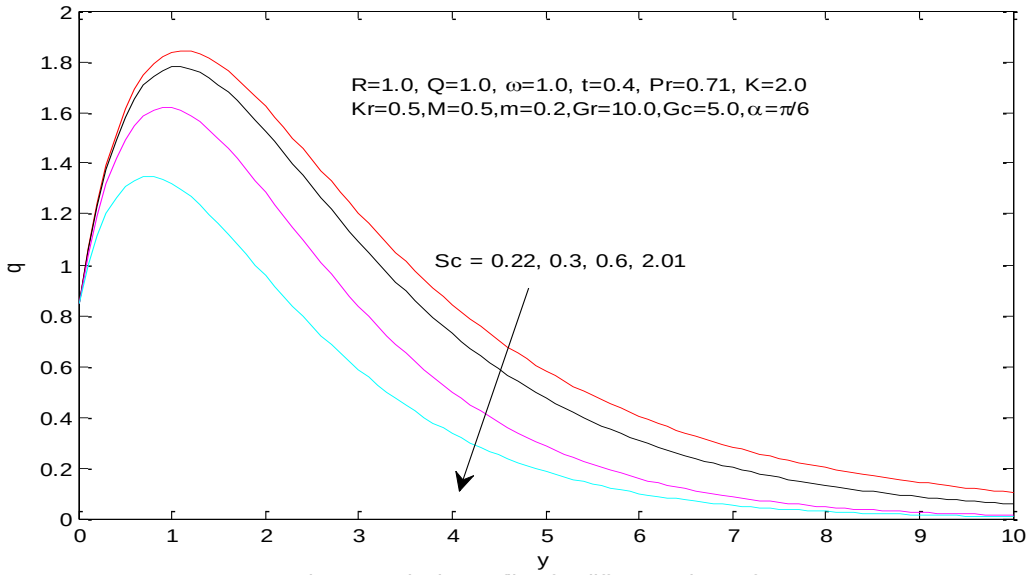

Fig. 12: Velocity profiles for different values of Sc

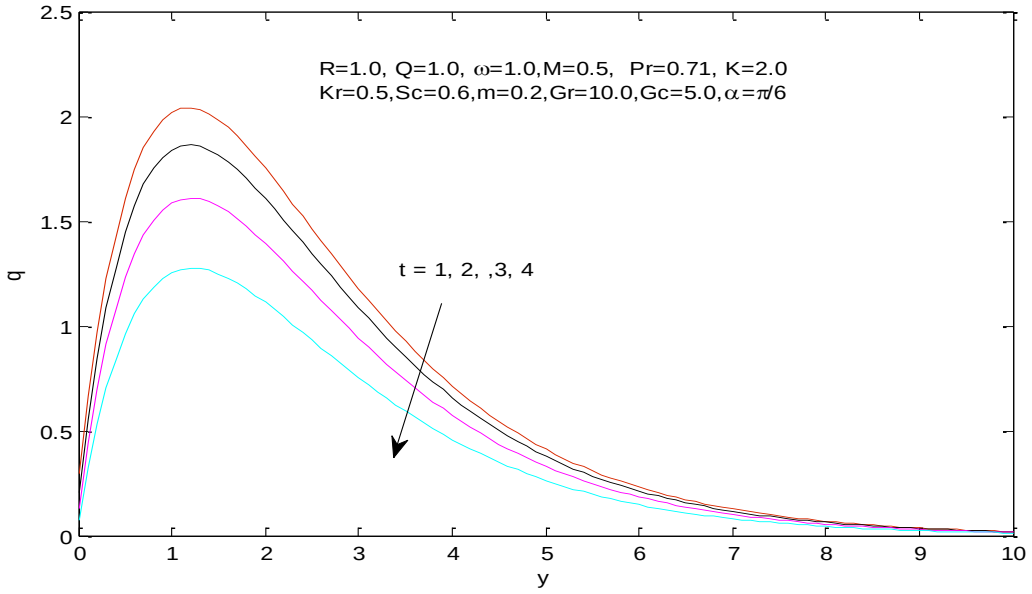

Fig. 13: Velocity profiles for different values of t

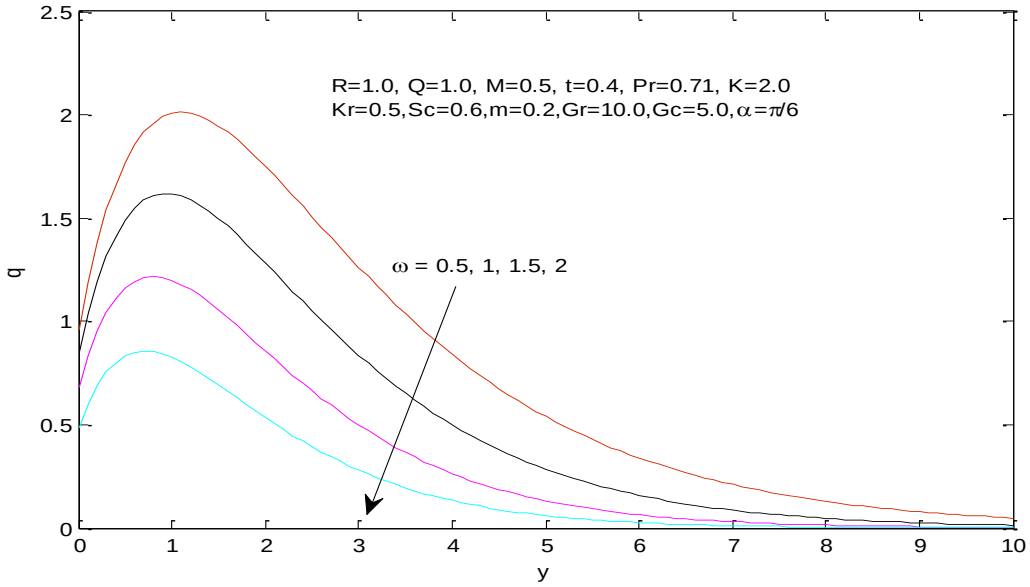

Fig. 14: Velocity profiles for different values of ω

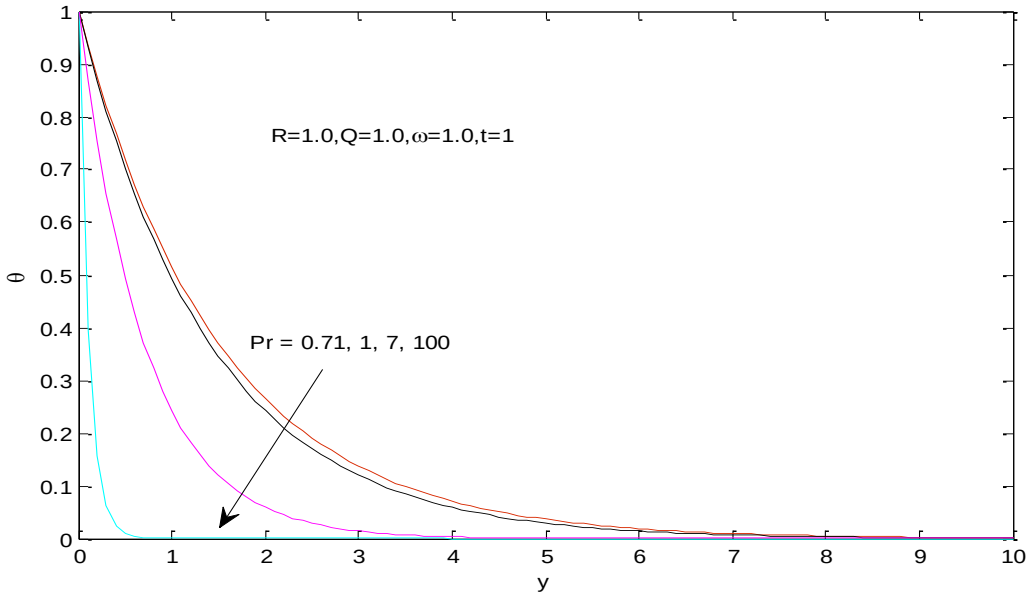

Fig. 15: Temperature profiles for different values of Pr

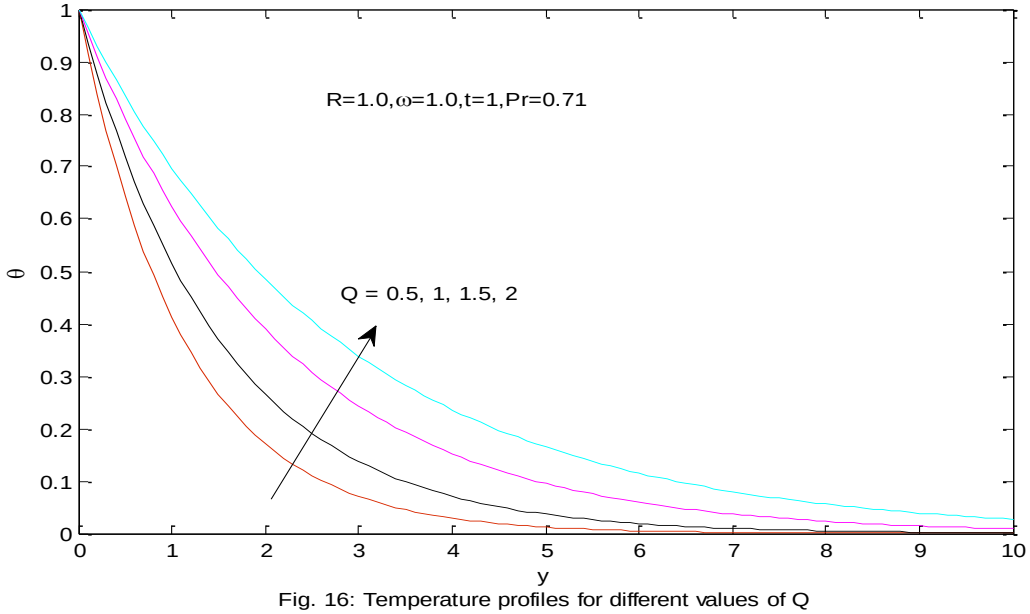

Fig. 16: Temperature profiles for different values of Q

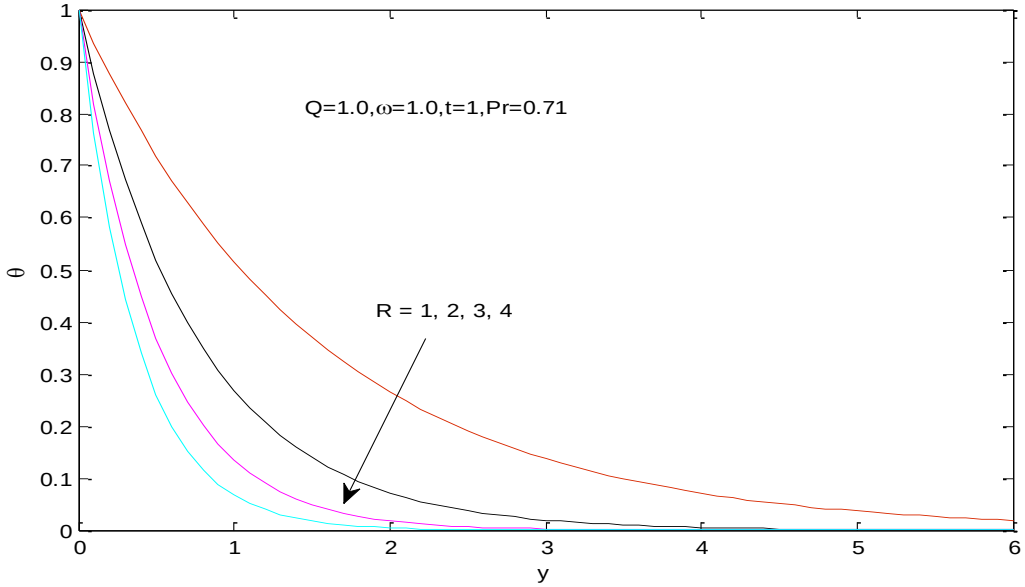

Fig. 17: Temperature profiles for different values of R

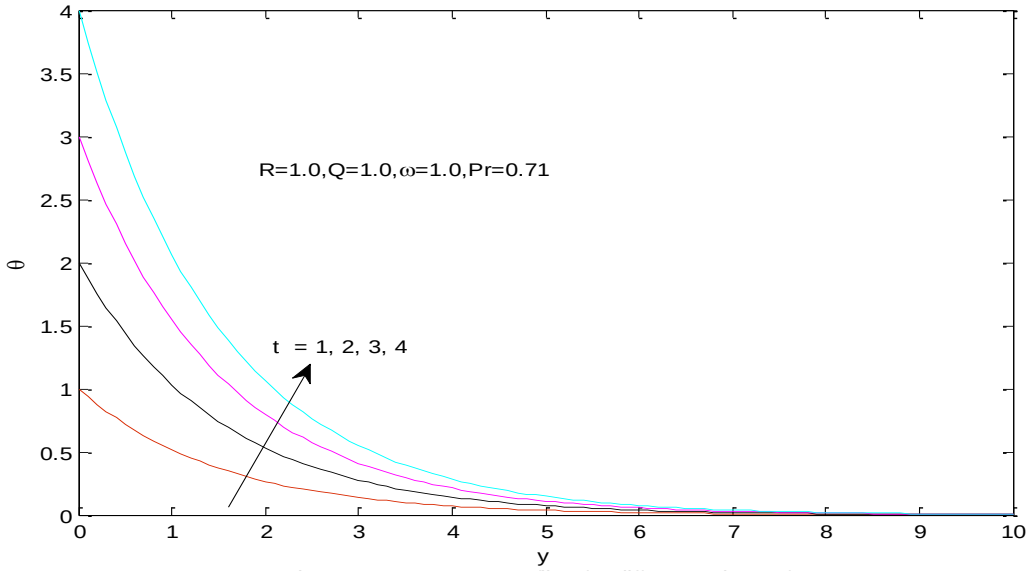

Fig. 18: Temperature profiles for different values of t

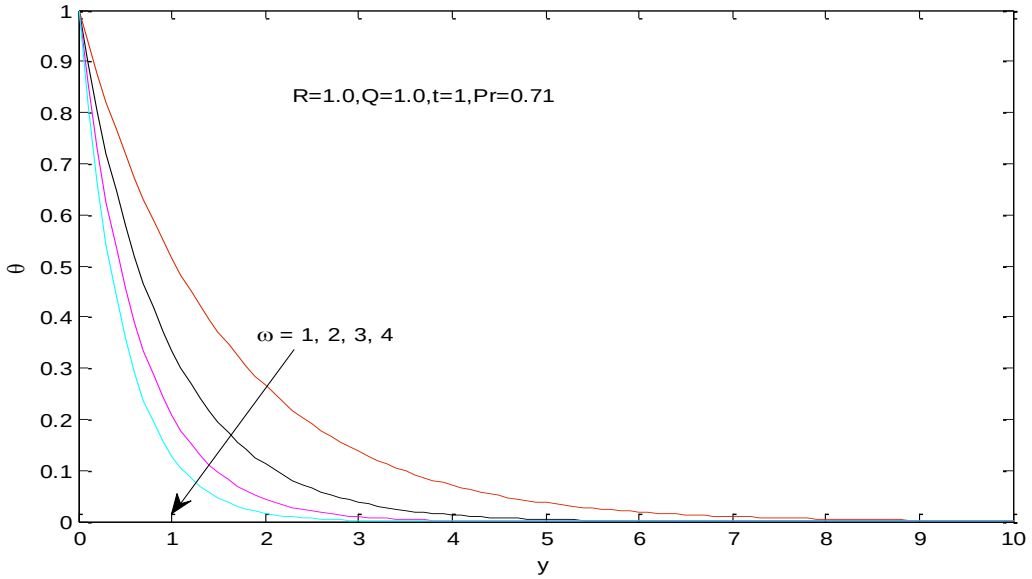

Fig. 19: Temperature profiles for different values of ω

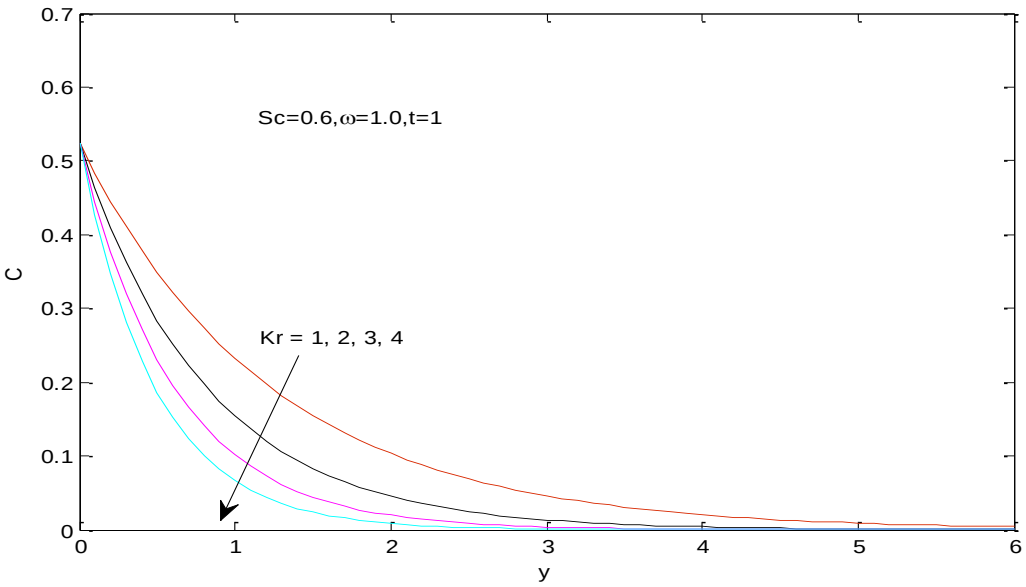

Fig. 20: Concentration profiles for different values of Kr

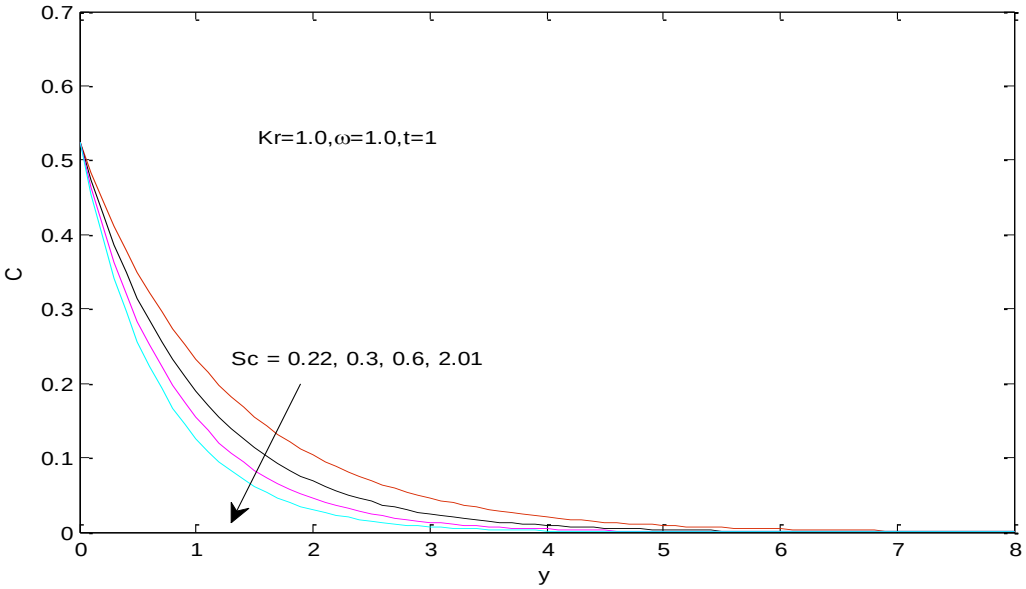

Fig. 21: Concentration profiles for different values of Sc

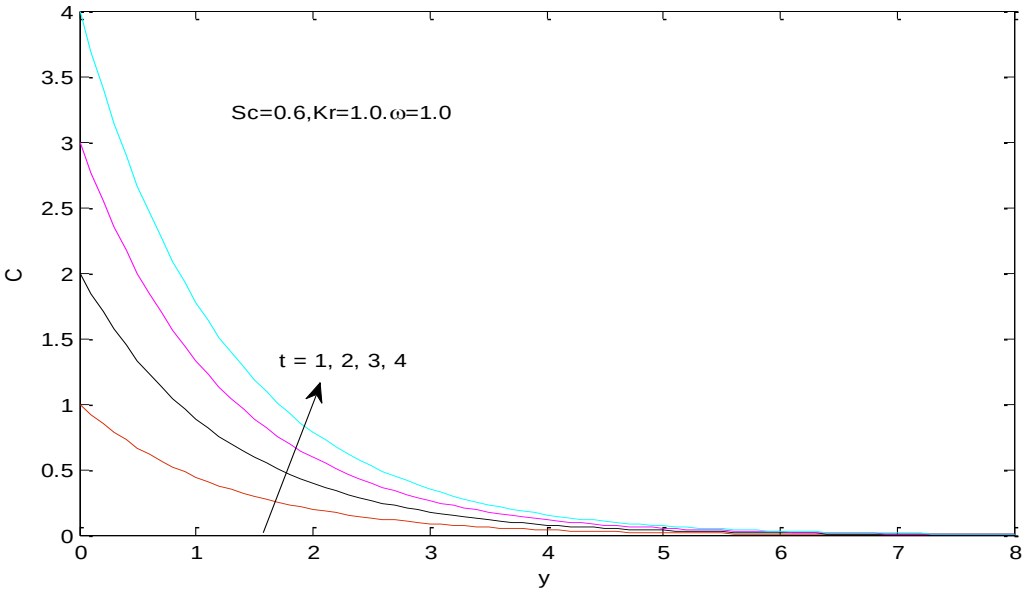

Fig. 22: Concentration profiles for different values of t

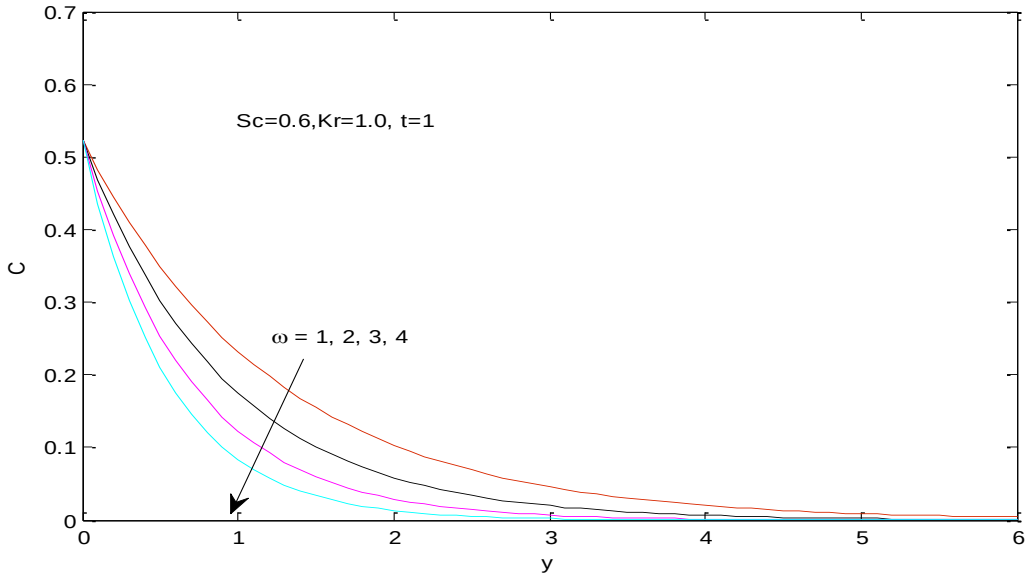

Fig. 23: Concentration profiles for different values of ω

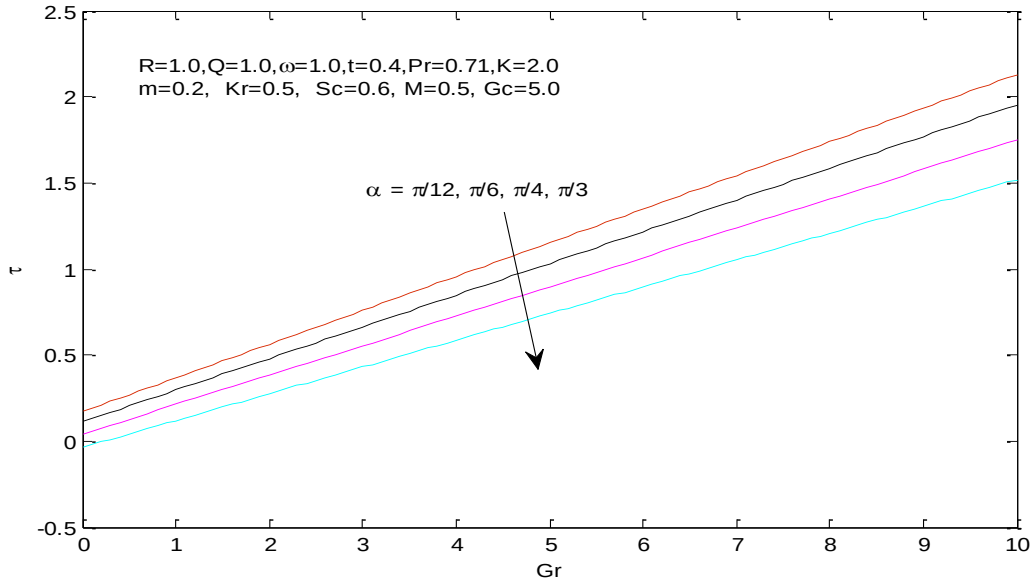

Fig. 24: Skin friction for different values of α

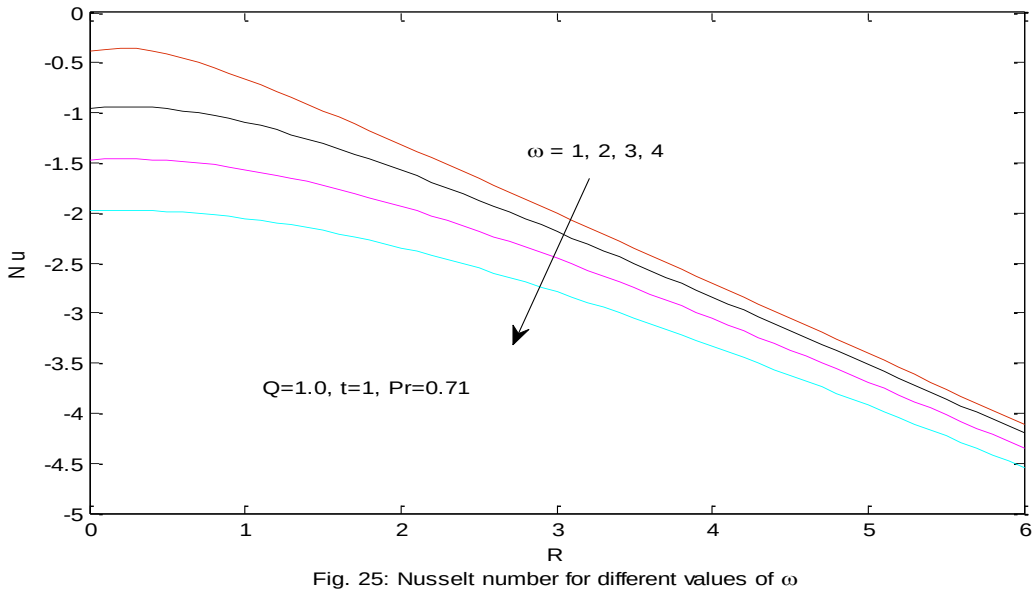

Fig. 25: Nusselt number for different values of ω

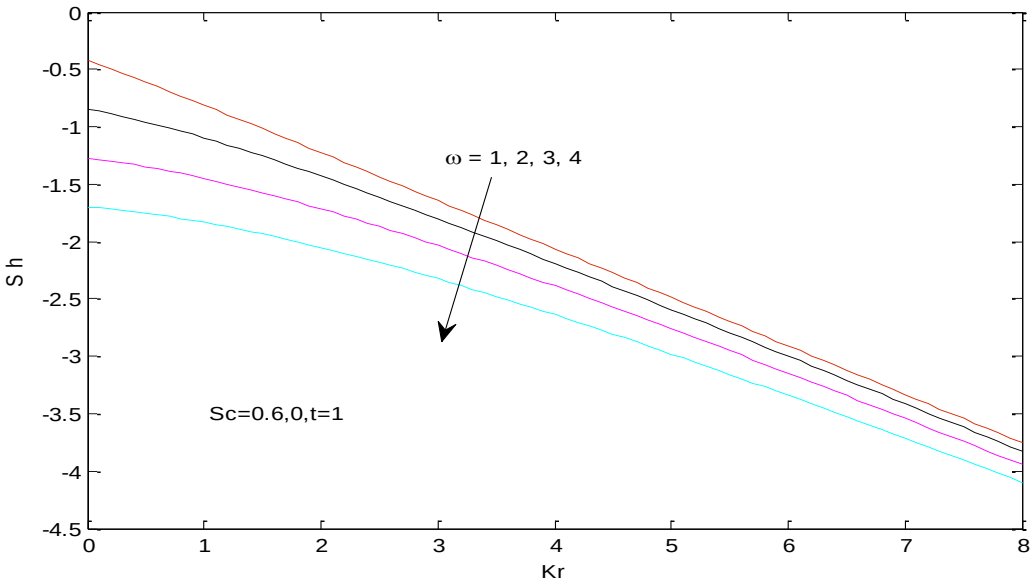

Fig. 26: Sherwood number for different values of ω